White Paper

SUSANNA LAURÉN, PHD
BIOLIN SCIENTIFIC

The Attension Theta Flex Optical Tensiometer with 3D Topography Module

Biolin Scientific
[Progress Together]

The Attension Theta Flex Optical Tensiometer with 3D Topography

In this white paper we will take an in-depth look at the principles underlying the 3D Topography Module method, resulting roughness parameters, and also the Wenzel theory used for roughness corrected contact angles. We will also highlight applications and samples that are feasible for this method.

Introduction

Measuring surface roughness together with contact angle makes it possible to separate the influence of surface chemistry from surface roughness on wetting and adhesion behaviour. This is especially important when working with different types of surface modifications where both surface chemistry and surface topography are altered.

Until now, contact angle and surface roughness have only been measured individually by using an optical tensiometer and a separate roughness measurement instrument. The Attension Theta Flex Optical Tensiometer with 3D Topography Module, see Figure 1, enables automated measurement of the surface roughness on the same sample location as the contact angle measurement by using automated XYZ sample movement. With the included software OneAttension, surface roughness and roughness corrected contact angles are calculated automatically.

Method description

Surface roughness measured with the Attension 3D Topography Module is based on structured lighting, where light patterns are projected onto a sample surface and the sample shape is analysed from images taken by a camera. Structured lighting has been used in various applications to measure 3D shapes at different length scales. In the 3D Topography Module, sinusoidal fringe patterns are used and thus the method is called sinusoidal fringe projection phase-shifting. With this method it is possible to simultaneously perform 2D and 3D characterization at pixel-level resolution.

As illustrated in Figure 2, the 3D Topography Module consists of a projector with an LED light source and a slide with sinusoidal fringe patterns on a grey-scale. These illumination patterns are sequentially projected onto the studied surface, and a digital camera captures the fringe patterns from which the 3D shape of the object is reconstructed by phase-shift coding. This enables pixel level measurement resolution. In the 3D Topography Module, the pixel

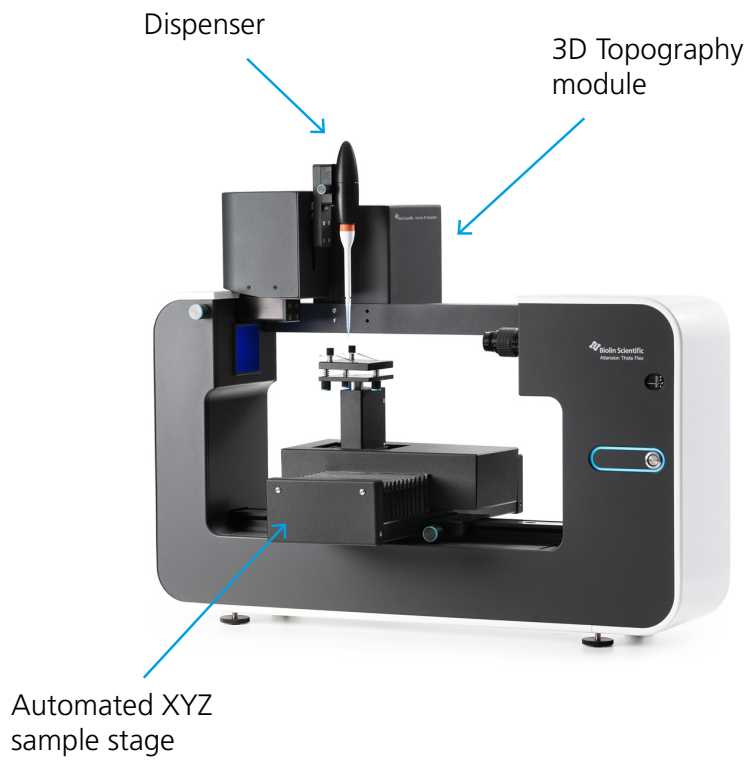

Figure 1
Attension Theta Flex Optical Tensiometer with 3D Topography Module

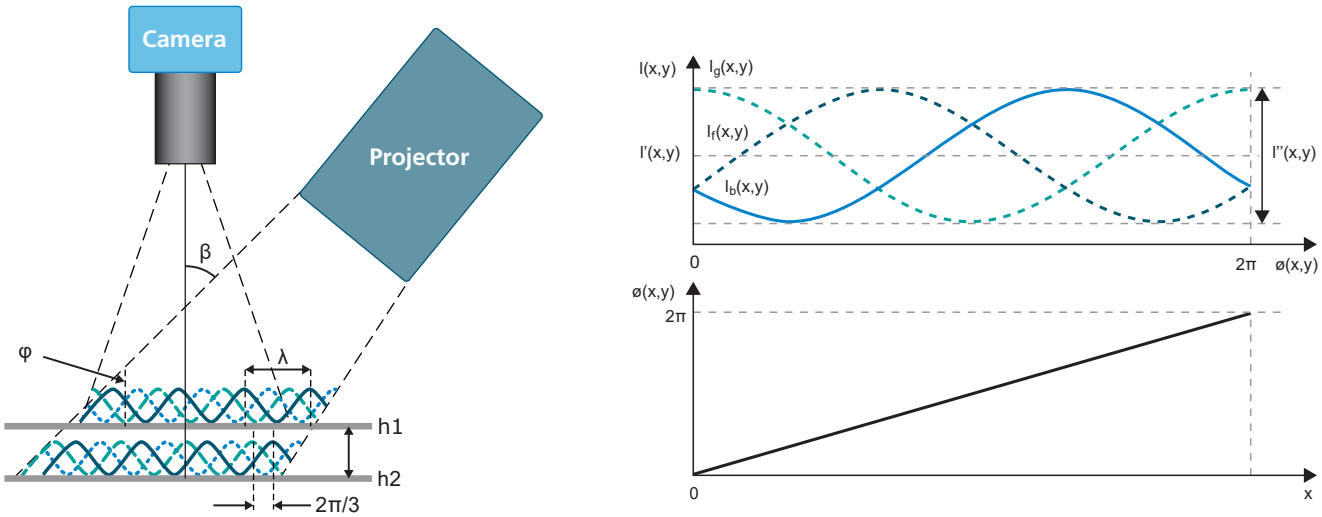

Figure 2

(Left) Fringe Projection Phase-Shifting shematics. A sinusoidal pattern is sequentially projected on the sample surface and a camera is utlized to capture the fringe patterns and recontruct the 3D image by phase-shift coding. (Right) In the sinusoidal phase-shifting method a series of phase-shifted sinusoidal patterns are recorded (top), from which the phase information at every pixel is obtained (bottom). The phase shift correlates with sample surface topography from pixel to pixel that defines the resolution.

size is 1.1 µm x 1.1 µm for analysis of micron-scale surface features.

The sinusoidal fringes can be expressed by:

$I_n(x,y) = a + b\cos(2\pi x/p + \varphi_0 + \delta_n)$

where (x, y) is the coordinate in the slide frame plane, a is background intensity, b is amplitude modulation, p is sinusoidal grating wavelength, φ_0 is the additional phase shift caused by the surface height and δ_n is the phase shift from the slide movement [1].

As an example for a color pattern with red, green, and blue light, we can demonstrate the case of three divided wavelengths where I_r, I_g, and I_b are the corresponding intensities for each of the colors. The phase shifts can be plotted as in Figure 2.

Then the spatial phase shift can be expressed with the following equation

The phase shift indicates the horizontal coordinate, i.e. the height differences in every pixel providing the sample topography.

There are many different algorithms available that use sinusoidal phase-shifting. For this application, the algorithm was based on an analogous grayscale version. The RGB light example is given to illustrate the principle, however the exact equations used in our approach are proprietary.

The algorithm and instrument design can be validated with a validation tool with a known surface structure. The validation specimen has a patterned structure with known surface topography features, allowing the user to compare the measured roughness value to a theoretical roughness value, see Figure 3.

Utilization of different roughness parameters

Surface roughness cannot be accurately characterized by using a single roughness parameter. Instead a set of surface roughness parameters are defined. Parameters that characterize surface profiles are called 2D parameters, and are marked with the letter "R". These parameters are widely utilized in different applications but are not really able to provide a complete picture for three dimensional surfaces. Parameters used to characterize the surface topog-

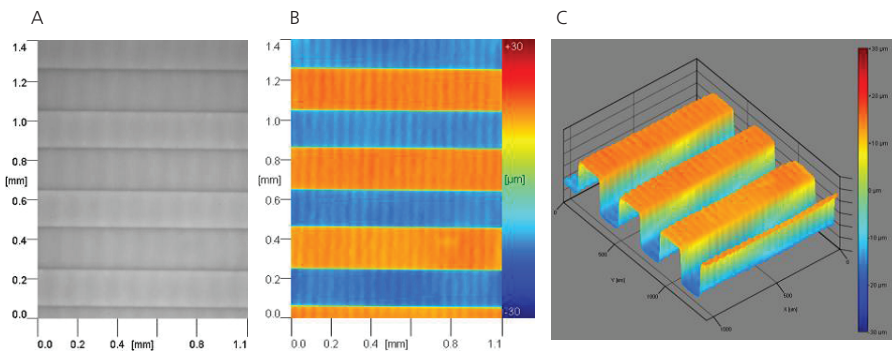

Figure 3

Attension 3D Topography Module images for the validation tool. A) optical image, B) 2D image and C) 3D image.

SYMBOL	NAME	EQUATION	DESCRIPTION
R_a, S_a	Arithmetic average	$S_a = \frac{1}{MN}\sum_{j=1}^{N}\sum_{i=1}^{M}\lvert\eta(x_i,y_j)\rvert$	Average of |z|
R_q, S_q	Root mean square (RMS) roughness	$S_q = \sqrt{\frac{1}{MN}\sum_{j=1}^{N}\sum_{i=1}^{M}\eta^2(x_i,y_j)}$	Standard deviation of z
R_p, S_p	Maximum height of peaks	$S_p = MAX\,(\eta_p)$	Max z
R_v, S_v	Maximum depth of valleys	$S_v = MIN\,(\eta_v)$	Min z
R_z, S_z	Maximum height of the surface	$S_z = (\lvert S_p\rvert + \lvert S_v\rvert)$	Max z- Min z
R_{10z}, S_{10z}	Ten point height	$S_z = \frac{\sum_{i=1}^{5}\lvert\eta_{pi}\rvert + \sum_{i=1}^{5}\lvert\eta_{vi}\rvert}{5}$	Average of five highest local maxima and five deepest local minima.
R_{sk}, S_{sk}	Skewness	$S_{sk} = \frac{1}{MNS_q^3}\sum_{j=1}^{N}\sum_{i=1}^{M}\eta^3(x_i,y_j)$	Height distribution asymmetry
R_{ku}, S_{ku}	Kurtosis	$S_{ku} = \frac{1}{MNS_q^4}\sum_{j=1}^{N}\sum_{i=1}^{M}\eta^4(x_i,y_j)$	Height distribution sharpness
S_{dr}	Area factor	$S_{dr} = \frac{(Textured\ surface\ area) - (Cross\ sectional\ area)}{Cross\ sectional\ area} * 100\%$ $= \frac{\sum_{j=1}^{N-1}\sum_{i=1}^{M-1}A_{i,j} - (M-1)(N-1)\Delta x\Delta y}{(M-1)(N-1)\Delta x\Delta y} * 100\%$	Ratio between the interfacial and projected areas

Table 1
The 2D and 3D roughness parameters measured with the 3D topography module.

raphy are called 3D parameters, and are marked with the letter "S". Some of the 3D parameters have 2D counterparts; others are specifically developed for 3D surfaces. A summary of these parameters as stated by the ISO 25178 standard (and their 2D counterparts) is presented in Table 1.

Only the area factor, S_{dr}, is utilized for the Wenzel contact angle roughness correction. However, with the 3D Topography Module a selection of 2D and 3D parameters are measured for detailed surface topographical characterization: S_a is the arithmetic mean height of the surface. S_q and its 2D counterpart are the most widely used roughness parameters that give the standard deviation of height. R_p and R_v give the maximum height of the summit and maximum depth of the valleys, respectively. R_z gives the peak to peak value and R_{10z} is calculated as the mean height value of five local maxima and local minima. It is worth pointing out that R_z is more sensitive to noise than R_{10z}. The ratio between the interfacial and projected area, S_{dr}, gives the additional surface area contributed by the texture. This parameter is especially useful in wettability studies since it can be used to calculate the roughness factor, r, utilized in the Wenzel equation.

The 3D Topography Module provides 3-dimensional characterization over a surface area of 1.4 mm x 1.1 mm. Larger surface areas up to 4.2 mm x 4.2 mm can be characterized by automatic stitching of images in OneAttension software.

Contact angle roughness correction by using Wenzel equation

Both chemical and topographical properties of the surface are important parameters in many different applications and processes, where wetting and adhesion behavior needs to be optimized. Wettability can be studied by measuring the contact angle of the substrate with a given liquid. The Young equation describes the balance at the three phase line between solid, liquid and gas:

$$\gamma_{sv} = \gamma_{sl} + \gamma_{lv}\cos\Theta_Y$$

The interfacial tensions, γ_{sv}, γ_{sl} and γ_{lv}, form the equilibrium contact angle of wetting, referred to Young's contact angle Θ_Y. Young's equation assumes that the surface is chemically homogenous and topographically smooth. This is however usually not true in the case of real surfaces, which instead of having one equilibrium contact angle value generally exhibit a range of contact angles between the advancing and receding values.

In Figure 4, a droplet on an ideal and a real surface is presented. On the ideal surface, Young's equation applies and the measured contact angle is equal to Young's contact angle (Figure 4A). On a real surface, the actual contact angle is the angle between the tangent to the liquid-fluid interface and the actual, local surface of the solid (Figure 4B). However, the measured (apparent) contact angle

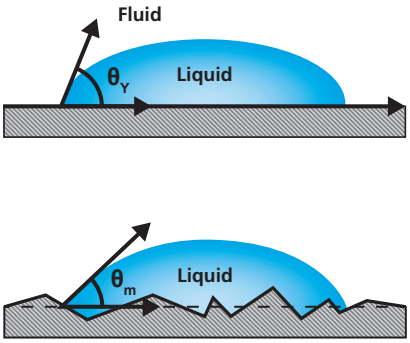

Figure 4

Definition of different types of contact angles; (A) Contact angle on an ideal surface is called the Young's contact angle (B) Apparent or measured contact angle on a real surface with an inherent roughness.

is the angle between the tangent to the liquid-fluid interface and the line that represents the apparent solid surface, as seen macroscopically. Actual and apparent contact angle values can deviate substantially from each other. To calculate theoretically valid surface free energies of the solid the actual contact angles should be used.

The relationship between roughness and wettability was defined in 1936 by Wenzel who stated that adding surface roughness will enhance the wettability caused by the chemistry of the surface. For example, if the surface is chemically hydrophobic, it will become even more hydrophobic when surface roughness is applied. Wenzel's statement [2,3] can be described by:

$\cos\Theta_m = r\cos\Theta_Y$

where Θ_m is the measured contact angle, Θ_Y is Young's contact angle and r is the roughness ratio. Roughness ratio is defined as the ratio between the actual and projected solid surface area (r=1 for a smooth surface and > 1 for a rough surface). It is important to note that the Wenzel equation is based on the assumption that the liquid completely penetrates into the roughness grooves (as in Figure 4B). Wenzel's equation is an approximation that becomes more accurate as the drop becomes larger compared to the scale of the roughness. It follows that if the drop is larger than the roughness scale by two to three orders of magnitude, the Wenzel equation applies. This fits well with contact angle measurement's length scale of microliter volume droplets being millimeters, and the roughness analysed by the 3D Topography Module being microns. The roughness ratio, r, for the Wenzel equation is calculated from the 3-dimensional area factor S_{dr} according to the following equation [4]:

$r = 1 + S_{dr}/100$

Applications

The 3D Topography Module is utilized in applications, where the micro-scale roughness is an important factor influencing a materials' adhesion properties.

Since the 3D Topography Module uses an optical method, a diffuse reflecting surface is required. Therefore, samples being completely black or transparent cannot be analysed. Also, surfaces with a mirror-like appearance (i.e. very shiny surfaces) may give irregular results.

Below examples of some application areas are given.

Biocompatibility of implants

Various materials such as metals, ceramics, and polymers, are being utilized as implants in medicine. The surface of the implant is typically modified to through mechanical roughning and/or chemical treatment to ensure biocompatibility with the surrounding host tissue. Separating the impact of chemical and mechanical treatment from water contact angles can be very useful in implant development and quality control. It has for example been studied how the chemical and mechanical surface treatment effects the wettability, surface roughness and surface free energy of ceramic materials used in clinical dentistry [5].

Paper and board coatings

Optimized wetting and adhesion to paper surfaces plays a crucial role in ensuring quality and runnability in various converting and finishing operations such as printing and packaging. Base paper can be coated for example with pigment coatings to provide a smooth surface for printing or by wax coatings to ensure a barrier against odor and gas transmission in packaging applications. Paper surfaces typically contain microscale roughness that has an influence on wetting and adhesion in addition to the applied coating chemistry. Thus, understanding the impact of roughness on wetting may help with coating formulation and optimization of surface treatment processes as well as to give more insight into the root cause of quality issues.

Other application areas

Coating and surface finishing for construction and building materials are important for enhanced appearance and durability. Adhesion of different types of coatings, such as paint or veneer sheeting can depend on both surface topography and surface chemistry. The Theta Optical Tensiometer with 3D Topography Module can be used for evaluating surface processing quality and its influence on wettability.

3D topography module has also been utilized in development of catalytic materials where high surface area of the material is typically needed [6-9].

Conclusions

In this white paper we have described the 3D Topography Module fringe projection phase-shifting principle, defined the roughness parameters measured with this method and shown how Wenzel's equation can be used to provide roughness corrected contact angles. In addition, a handful of the most common application areas, along with sample limitations have been described.

References

1. S. Zhang, and P. Huang, "High-resolution, real-time 3D shape acquisition", Computer vision and pattern recognition Workshop 2004.
2. A. Marmur, "Soft contact: Measurement and interpretation of contact angles", Soft Matter 2 (2006) 12.
3. R.W.Wenzel, "Resistance of solid surfaces to wetting by water", Industrial & Engineering Chemistry 28 (1936) 988.
4. J. Peltonen, M. Järn, S. Areva, M. Linden, and J.B. Rosenholm, "Topographical parameters for specifying a three-dimensional surface", Langmuir 20 (2004) 9428.
5. R.B.W. Lima, S.C. Barreto, N.M. Alfrisany, T.S. Porto, G.M. De Souza, and M.F. De Goes, "Effect of silane and MDP-based primers on physico-chemical properties of zirconia and its bond strength to resin cement", Dental Materials 35 (2019) 1557.
6. E. Das, B.Y. Kaplan, S.A. Gursel, and A.B. Yurtcan, "Graphene nanoplatelets-carbon blacn hybrids as an efficient catalys support for Pt nanoparticles for polymer electrolyte membrane fuel cells", Renewable energy 139 (2019) 1099.
7. A.B. Yurtcan, and E. Das, "Chemically synthesized reduced graphene oxide-carbon black based hybrid catalyst for PEM fuel cells", International journal of hydrogen energy 43 (2018) 18691.
8. B. Hui, K. Zhang, Y. Xia, and C. Zhou, "Natural multi-channeled wood frameworks for electrocatalytic hydrogen evolution", Electrochimica Acta 330 (2020) 135274.
9. J. Lyu, G. Sun, L. Zhu, H. Ma, C. Ma, X. Dong, and Y. Fu, "Fabrication of Ti/black TiO2-PbO2 micro/nanostructures with tunable hydrophobic/hydrophilic characteristics and their photoelectrocatalytic performance", Journal of solid state electrochemisty 24 (2020) 375.